Cardiovascular Toxicology (2019) 19:529–547
https://doi.org/10.1007/s12012-019-09527-8

Acylated Ghrelin Protects the Hearts of Rats from Doxorubicin-Induced Fas/FasL Apoptosis by Stimulating SERCA2a Mediated by Activation of PKA and Akt

Ali A. Shati[1] · M. Dallak[2]

Published online: 15 May 2019

Abstract
This study investigated if the cardioprotective effect of acylated ghrelin (AG) against doxorubicin (DOX)-induced cardiac toxicity in rats involves inhibition of Fas/FasL-mediated cell death. It also investigated if such an effect is mediated by restoring Ca^{+2} homeostasis from the aspect of stimulation of SERCA2a receptors. Adult male Wistar rats were divided into 4 groups (20 rats/each) as control, control + AG, DOX, and DOX + AG. AG was co-administered to all rats consecutively for 35 days. In addition, isolated cardiomyocytes were cultured and treated with AG in the presence or absence of DOX with or without pre-incubation with [D-Lys3]-GHRP-6 (a AG receptor antagonist), VIII (]an Akt inhibitor), or KT-5720 (a PKA inhibitor). AG increased LVSP, dp/dt_{max}, and dp/dt_{min} in both control and DOX-treated animals and improved cardiac ultrastructural changes in DOX-treated rats. It also inhibited ROS in control rats and lowered LVEDP, intracellular levels of ROS and Ca^{2+}, and activity of calcineurin in LVs of DOX-treated rats. Concomitantly, it inhibited LV NFAT-4 nuclear translocation and downregulated their protein levels of Fas and FasL. Mechanistically, in control or DOX-treated hearts or cells, AG upregulated the levels of SERCA2a and increased the activities of PKA and Akt, leading to increase phosphorylation of phospholamban at Ser^{16} and Thr^{17}. All these effects were abolished by D-Lys3-GHRP-6, VIII, or KT-5720 and were independent of food intake or GH/IGF-1. In conclusion, AG cardioprotection against DOX involves inhibition of extrinsic cell death and restoring normal Ca^{+2} homeostasis.

Keywords Ghrelin · Doxorubicin · Fas ligand · Ca^{+2} · NFAT

Introduction

It is now well accepted that the overproduction of reactive oxygen species (ROS) and intracellular calcium $[Ca^{2+}]i$ overload are the key players in doxorubicin (DOX)-induced cardiomyocytes apoptosis and the subsequent irreversible heart failure (HF) in cancer patient and intoxicated animal [1–3]. Currently, accumulating evidence has shown that apoptosis mediated by the extrinsic [Fas/Fas Ligand (Fas/FasL)-mediated] cell death is prominent over that of the intrinsic (mitochondria-mediated) cell death during progression to HF, post-DOX-therapy [1, 4–7]. Indeed, DOX rendered the cultured cardiomyocytes more sensitive to Fas/FasL-induced apoptosis by overexpression of Fas receptor [7]. It also enhanced expression of FasL and induced Fas/FasL cell death by Ca^{2+}-dependent activation of calcineurin-induced activation and nuclear translocation of nuclear factor of the activated T cells-4 (NFAT4), a major trans-coactivator of FasL promoter [5].

Hence, and during the recent decades, much attention was given to understand the mechanisms by which DOX increases $[Ca^{2+}]i$ with a belief that blocking this event may provide a novel strategy to maintain heart contractility and protect the cardiomyocytes from the associated extrinsic cell death. Sarcoplasmic reticulum Ca^{2+} pump-2a (SR Ca^{2+}-ATPase2a or SERCA2a) is the major Ca^{+2} pump in the heart of mammles that regulates mobilization of Ca^{+2} ions during the cardiac cycle and plays an essential role during cardiac contractility as it is indispensable for

Handling Editor: Bérengère Dumotier.

✉ Ali A. Shati
aaalshati@kku.edu.sa

[1] Department of Biology, College of Science, King Khalid University, Abha, Saudi Arabia

[2] Department of Physiology, College of Medicine, King Khalid University, Abha, Saudi Arabia

resequestering Ca^{2+} to SR during relaxation [8]. Interestingly, among all cardiac Ca^{2+} regulatory proteins, SERCA2a levels were significantly reduced in the failing hearts of animals and human of various cardiac diseases [9, 10]. The activation of SERCA2a is associated with an increase in $[Ca^{+2}]i$ during diastole, decreased contractility, and activation of the calcium-/calcineurin-dependent complex [9–12]. Similarly, reduced levels of SERCA2a were also observed in the failing hearts or cultured cardiomyocytes after DOX treatment mediated by activation of Erg-1, a common cellular inhibitor of SERCA2a promoter [13–15].

SERCA2a activity is correlated with mRNA and protein levels of the pump [14]. In addition, cardiac SERCA2a activity is tightly regulated and enhanced by phosphorylation activation of an associated membrane protein, phospholamban (PLB) [16, 17]. In the heart, phosphorylation of PLB is induced by the activation of Protein Kinase A (PKA) (at Ser^{16}) and Ca^{2+}/calmodulin-dependent protein kinase II (CaMKII) (at Thr^{17}) [18]. Also, other studies have shown that activation of protein kinase B (Akt) phosphorylates PLB at Ser^{16} and Thr^{17} and it may act as an upstream inducer of PKA [19–21]. Level of PLB remained unaffected, but its phosphorylation rate was reduced and correlated with the reduced activity of SERCA2a. However, although one study has shown that DOX may reduce cardiac PLB level during the development of HF [22], there is no definite clear effect of DOX on PLB level and phosphorylation.

On the other hand, recent studies have shown a cardioprotective effect of endogenous and exogenous acylated ghrelin (AG) in healthy men and animals, as well as, in patients or animals with myocardial infarction (MI), ischemia/reperfusion injury and HF [23, 24]. This has been supported by the presence of mRNA of both AG and its receptor, growth hormone (GH) secretagogue receptor-a1 (GHSRa1), in the hearts of animals and human [23, 25, 26]. Acylated ghrelin have a wide range of action on the cardiovascular system including a vasodilator effect, improvement of cardiac contractility and antioxidant defense, and inhibition of apoptosis and cardiac remodeling [23, 24, 27, 28]. The protective role of AG against DOX-induced cardiomyocytes apoptosis has been also reported in vitro, as it is able to increase numerous cell survival pathways (PI3K/Akt) and inhibit Fas agonist-induced extrinsic cell death [27, 28]. However, the effects of AG on DOX-induced alterations in Ca^{+2} homeostasis and Fas/FasL have not been investigated in vivo.

Interestingly, it was shown that AG inhibited Angiotensin II-induced increase in the Ca^{+2} concentration in vascular smooth muscle by activating PKA [29]. In addition, the anti-apoptotic effect of AG in various tissues including the heart was mediated by activation of Akt [27, 30]. These findings prompted us to hypothesize that AG may inhibit DOX-induced Fas/FasL-mediated cell death by activating SERCA2a activity through increased phosphorylation of PBL. However, it may act by other methods.

Therefore, the main aim of this study was to investigate if chronic administration of AG could protect the hearts of rats against DOX-induced Fas/FasL cell death and HF. This study also aimed to investigate if such protection is mediated by restoring normal Ca^{2+} homeostasis with a focus on its effect on SERCA2a expression level, phosphorylation of PBL, and activities of PKA and Akt.

Materials and Methods

Animals

Adult male healthy Wistar rats weighing 140 ± 5 g, 8 weeks of age were used the experimental procedure. All rats were obtained and housed at the animal house of King Khalid University (KKU), Abha, Saudi Arabia, in a single room under a temperature of 22 ± 1 °C, humidity of 60%, and a 12 h light/dark cycle and had free access to their control chow and drinking water. All procedures used in this study were approved by the College of Science Ethical Committee for the use and care of laboratory animals which follows the recommendations for the use and care of laboratory established by the US National Institutes of Health (NIH publication No. 85-23, revised 1996).

Experimental Design

Eighty rats were divided into 4 groups (n = 20, each as follows: (1) control group: administered 0.2 ml of normal saline (s.c.) for 5 weeks on a daily basis, (2) AG-treated group: administered (s.c.) 0.2 ml of synthetic rat AG (cat. no. G8903.1MG; Sigma Aldrich, UK) in a final dose of 10 ng/kg for 5 consecutive weeks, every 20 h. (3) DOX-treated rats: administered DOX in an accumulative final dose of 15 mg/kg over a period of 2 weeks on alternate days (2.5 mg/kg, i.p/dose, 6 doses) according to the procedures established by Lou et al. [31]. These rats were also administered normal saline (0.2 ml, s.c.) from the first day of DOX therapy until the end of day 35, and (4) DOX + AG-treated rats: administered DOX as mentioned above for 2 weeks and coadministered AG (10 ng/kg) (every 20 h), starting from the first dose of DOX, until the end of day 35. The experimental procedures were stopped by the end of day 35 as shown that such protocol results in HF 3 weeks after the last dose [31]. A summary of the experimental design is shown in Fig. 1.

In addition to the above-mentioned groups, we have also included another control group which was administered the vehicle (0.2 ml, i.p) at 6 doses on alternate days over 2 week period to match DOX-treated groups. However, as no death occurs in these rats and all measured parameter in

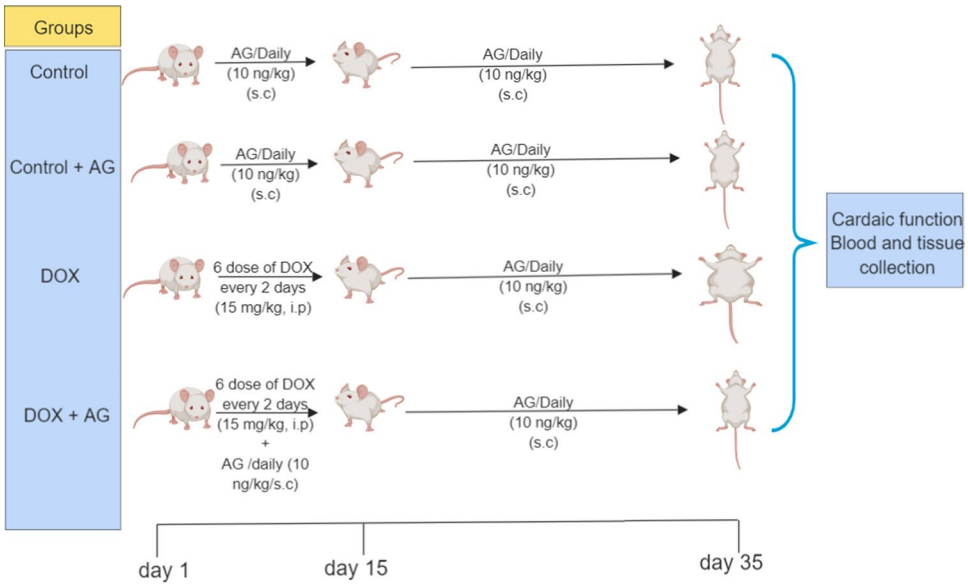

Fig. 1 A summary of the experimental design of this study

this control group were not significantly different from the control groups which received the vehicle, s.c., this group was omitted for simplicity.

Dose Selection

Previously, it was shown that normal AG in fasting rats is about 100 pg/ml [32]. The dose of AG used in this study was selected after a series of preliminary experiments to cause a sustained increase in circulatory AG to a supra-physiological level (around 150 pg/ml that is sustained for the next 20 h). Also, this dose was also able to restore circulatory levels of AG in DOX-treated rats to almost normal levels (shown in the results). Given that the adult rat used in this study are averaged about 140 g (1 kg/7.41) and contain an averaged blood volume of 20 ml, then 10 ng/ml which is equivalent to 1000 pg/ml was be divided over 7.14 and then over 20 ml. So, the equivalent dose was about 70 mg/ml of blood. Such dose was also used by other authors to yield a supra-physiological level and was associated with a potent antioxidant and anti-inflammatory effects with no effect on food intake or body weights in control rats [33, 34].

Biochemical Analysis in the Serum

Twelve hours post the last treatment on day 35, 1 ml blood was collected from rat's tail into EDTA-tubes (in some cases into special tubes supplied with the kit used to measure levels of AG), centrifuged at 3000 rpm for 10 min to collect plasma. Samples were stored at − 20 °C for further biochemical analysis. Plasma levels of creatine kinase-MB (CK-MB) and brain natriuretic peptide (BNP) were analyzed using commercial rat's ELISA kits (cat. no. E4608, Biovesion, USA & cat. no ab108816, Abcam, UK, respectively). Plasma levels of AG were measured within 3 days after blood collection using special rat's ELISA kits (A05117, SPI Bio, France). The kit is already provided with collecting tubes, protease inhibitors and chemical reagents to prevent AG degradation and promote its stabilization. All samples were measured in duplicates for 12 samples/group in accordance with the manufacturer's instructions. After blood collection, all rats were then returned to their cages for the next 24 h with free access to food and water uptake.

Recording of Cardiac Hemodynamic Parameters and Tissue Collection

Twenty-four hours after blood collection, left ventricular systolic pressure (LVSP), left ventricular end-diastolic pressure (LVEDP), maximal rate of increase in LV pressure ($LVdP/dt_{max}$), and maximal rate of decrease in LV pressure ($LVdP/dt_{min}$) were recorded in all rats of all groups, in an open chest surgery, at the physiology laboratory at the College of Medicine at KKU, Abha, KSA, according to their pre-established method [24]. All recordings were performed for 30 min after an initial stabilization period of 10 min and were acquired and analyzed using LabChart software and blood pressure analysis module (V8, AD Instruments Ltd., Australia). At the end of the recording, LVs were directly removed and rapidly washed with ice-cold phosphate buffered saline (PBS, pH 7.4). Then, they were cut on ice into smaller pieces, some of which were frozen at − 80 °C for biochemical and molecular analysis studies and other parts were fixed in 2.5% glutaraldehyde prepared in 0.1 M sodium cacodylate buffer and processed for electron microscopy studies.

Preparation of Whole Cell, Cytosolic, and Nuclear Fractions

To prepare the total cell homogenate, frozen LVs samples (30 mg) were homogenized, individually, in 0.5 ml of ice-cold phosphate PBS (pH 7.4) supplied with protease and inhibitors cocktail (cat. no. P8340 Sigma-Aldrich, MO, USA). The resultant supernatants were stored at − 80 °C and used later for the measurements of some biochemical parameters. The nuclear and cytoplasmic fractions were prepared from frozen LVs using a commercially available kit (cat no. 78835, ThermoFisher Scientific). These fractions were stored at − 80 °C and used later for western blotting detection of NFAT4.

Measurements of Biochemical Parameters in LV Homogenates

The activity of calcineurin in the cardiac homogenates or cultured cells was determined using a calcineurin cellular activity assay Kit (cat. no. BML-AK816, Enzo Life Sciences, Lausen/Switzerland). Levels of total ROS in LVs homogenates were measured using an OxiSelect™ in vitro assay kit (cat. no. STA-347, Cell Biolabs, Inc. San Diego, CA). Levels of intracellular Ca^{2+} in the LVs homogenate or cultured cells were measured using Flou-8 calcium flux assay kit (ab112129, Abcam UK). Absorbance or the fluorescence intensity was measured using Paradigm Detection Platform (Beckman Coulter) at the provided wavelengths or excitation and emission wavelengths. All procedures were done for n = 6/group and presented as percentages of control.

LV Cardiomyocyte Isolation and Culture

For the in vitro part of the study, LV cardiomyocytes were isolated from adult healthy male Wistar rats (with the same genetic background to those used in the in vivo part) as exactly described by Donthi et al. [35]. Then, cardiomyocytes were counted and cultured (3×10^5) for 24 next hours at 37 °C (95% air, 5% CO_2) in 25-cm^2 culture flasks containing 5 ml of culture Dulbecco's modified Eagle's (DMEM) medium containing 10% fetal bovine serum (FBS), 0.1 mg/ml streptomycin, and 100 U/ml penicillin (Sigma Aldrich UK). During the procedure, the content of each flask was decanted into a new flask at 4 and 24 h after the initial culture to remove fibroblast. Then, the medium was changed after 4 days and then every other day thereafter.

Cardiomyocytes Treatments

Experiments involving cultured cardiomyocytes were performed in 60 mm culture dishes. DOX and AG were prepared directly in PBS whereas all other inhibitors (Sigma Aldrich, UK) were prepared in dimethylsulfoxide (DMSO) and then diluted in PBS (DMSO final concentration was 0.1%). Cells were incubated in the culture media with DOX (1 μM) in the absence or presence of AG (1 μM) for 20 h. To investigate if the effect of AG mediated by GHSRa1, Akt, and PKA, some cells were pre-incubated with either AG receptor antagonist ([D-Lys3]-GHRP-6; 10 μM), Akt inhibitor (VIII; 20 μM), or PKA inhibitor (KT-5720; 5 μ) for 2 h before being re-incubated in new media contains DOX and AG. Control cells were incubated with DMSO alone. The concentration of DOX, AG, and all other inhibitors used in this study were adopted from similar studies [27, 36–38]. Cell viability in cultured cells was performed using MTT assay (tetrazolium blue thiazol-3-[4,5-dimethylthiazol-2-yl]-2,5-diphenyl-tetrazolium).

Quantitative Real-Time PCR (qPCR)

mRNA levels of SERCA2a, IGF-1, GHSRa1, and GAPDH were measured using qPCR. Primer pairs for the above-mentioned genes were adopted from similar studies in Wistar rats [30, 39, 40] and are shown in Table 1. Briefly, total RNA was extracted from each LV sample (50 mg) using RNeasy Mini Kit (cat. no. 74104, Qiagen, Victoria, Australia). Single-stranded cDNA was synthesized using Superscript II reverse transcriptase and oligo (dT) (cat. no. 18064014, ThermoFisher, MA, USA). PCR runs were performed a CFX96 real-time PCR system (Bio-Rad, CA, USA) using Ssofast Evagreen Supermix (cat. no. 172-5200, BioRad, Montreal, Canada). Each plate contained at least two controls without template DNA. All procedures were done in duplicates for n = 6/group and according to the manufacturer's instructions.

Table 1 Primers used in the PCR reaction

Gene	Genbank acc. no.	Forward (5′=>3′)	Reversed (5′=>3′)	Product size (bp)
SERCA2a	AY-948198	GGAGGCGTTGCTAAACACTC	GAACCAGCCTTCGATATTGG	201
GHSRa1	U94321	AGGCAACCTGCTCACTATGCTG	GACAAGGATGACCAGCTTCAGC	292
IGF-1	NM 001082477	AAGCCTACAAAGTCAGCT CG	GGTCTTGTTTCCTGCACTTC	166
GAPDH	NM_017008	ACCCATCACCATCTTCC	GGTTCACACCCATCACA	194

Western Blotting

To prepare total homogenates, frozen LVs or isolated cultured cardiomyocytes of all groups were homogenized in 0.5 ml RIPA buffer (150 mM sodium chloride 1.0% NP-40 or Triton X-100 0.5% sodium deoxycholate 0.1% SDS, 50 mM Tris, pH 8.0) plus protease inhibitors (cat. no. P8340, Sigma-Aldrich, St. Louis, MO, USA). Protein levels of NFAT4 were determined in both the nuclear and cytosolic fraction prepared from LVs as previously mentioned above, whereas all other proteins were detected in the total cell extracts. In all cases, protein levels in all fractions were measured using a Pierce BCA Protein Assay Kit (cat. no. 23225, ThermoFisher Scientific). For western blotting, an equal amount of proteins (60 µg/well) were loaded and resolved on an SDS–polyacrylamide gel (8–12%) and then electroblotted onto nitrocellulose membranes (Sigma Aldrich UK). After successful washing with Tris-buffered saline (TBS-T) and blocking with 5% nonfat milk (in TBS-T buffer), membranes were incubated with the primary antibody as shown in Table 2. Membranes were then incubated with the corresponding HRP-conjugated secondary antibody. All antibodies were diluted in TBS-T buffer (Table 2). Antigen–antibody-interactions were detected using a Pierce ECL kit (ThermoFisher, USA, Piscataway, NJ) and then photographed and analyzed by C-DiGit Blot Scanner (LI-COR, USA) and its associated software. Each membrane was stripped up to 4 times in which the detection of phosphorylated form was done first and the detection of β-actin was the last. Data were analyzed for at least three samples/group or treatment. Band density between gels and the stripped blot was normalized using an internal standard.

Electron Microscopy Evaluation

For electron microscopy, LVs were fixed in 2.5% glutaraldehyde prepared in 0.1 M sodium cacodylate buffer for 24 h followed by embedment in Spur's resin and cut into 1 µm semi-thin sections. Ultrathin sections were then stained with uranyl acetate and lead citrate followed by examination with a JEM-1011transmission electron microscope, Jeol Co. Japan at 80 kV.

Statistical Analysis

All data were analyzed using GraphPad Prism statistical software package (version 6) using one-way analysis of variance (One-Way ANOVA) followed by Tukey's test for multiple comparisons. $p > 0.05$ was considered significantly different and values were presented as mean ± SD.

Results

General Observation

We have monitored the general appearance of rats of all groups during the time course of this study. Generally, at the end of week 2 of DOX-treatment (the last dose of DOX), DOX-treated animals looked sick, lethargic and their hair became scruffy with yellow tings and slightly enlarged abdomens, compared to all other groups. However, all other groups looked healthy and energetic. These symptoms became more extensively and profound with time in DOX-treated rats, as animals developed large abdomens and ascites during the 2nd and 3rd week post the last DOX-injection. At the time of dissection or necropsy (at time of death), livers of control or control + AG-treated rats

Table 2 Antibodies used in the current study

Antibody	Ca. no.	MW (kDa)	Manufacturer
SERCA2a	sc-53010	100, 1:100	Santa Cruz Biotechnology
Phospholamban (PBL)	14562	12/24, 1:1000	Cell signalling Technology
p-PLB (Ser^{16})	PA1-25784	6, 1:250	ThermoFisher Scientific
p-PLB (Thr^{17})	A010-13AP	27, 1:100	Badrilla
NFAT4 (NFATc3)	4998	140–190, 1:500	Cell signalling Technology
Fas	sc-74540	48 kDa, 1:1000	Santa Cruz Biotechnology
FasL	sc-19681	26/40 kDa, 1000	Santa Cruz Biotechnology
Caspase-12		15, 1:500	Santa Cruz Biotechnology
Akt	sc-5298	62: 1:1000	Santa Cruz Biotechnology
p-Akt (Ser^{473})	9271	60, 1:500	Cell signaling Technology
PKA	4782	42,1:500	Cell signaling Technology
p-PKA (Thr^{197})	4781	42, 1:500	Cell signaling Technology
Cleaved caspase-3	9661	1/19, 1:500	Cell signalling Technology
B-actin	4967	45, 1:3000	Cell signalling Technology

appeared normal with no peritoneal fluid accumulation. However, DOX-treated rats had enlarged dark color livers and increased volume of peritoneal fluids in their abdomens, whereas DOX + AG-treated rats showed almost normal livers appearance with very little to no fluid accumulation in their abdomens (volumes not measured).

Changes in Body Weights, Food Intake, and Survival Rate

Plasma levels of AG and average food intake measured between week 1 and week 5 as well as final body weight were significantly decreased in DOX-treated rats compared to control rats (Fig. 2a–c). However, plasma AG was slightly but significantly increased in DOX + AG-treated rats during the first 2 weeks of therapy (Fig. 2a). On the other hand, levels of AG have significantly increased overall periods of the study in the control + AG-treated rats compared to control rats (Fig. 2a). Administration of AG to control or DOX-treated rats didn't significantly alter their food intake or final body weights compared to control or DOX-treated rats, respectively (Fig. 2b and c). In addition, with no death was recorded in control + AG-treated rats, the survival rate was significantly decreased in DOX-treated rats (7 deaths) and was significantly reduced to 3 deaths only in DOX + AG-treated rats (Fig. 2d).

Changes in Plasma Cardiac Markers and Hemodynamic Parameters

Plasma levels of CK-MB and BNP 45 and values of LVEDP were not significantly changed but values of LVSP, $dp/dt_{max,}$ and dp/dt_{min} were significantly increased in control + AG-treated rats compared to control group (Fig. 3a–d). However, levels of CK-MB and BNP 45 and values of LVEDP were significantly increased whereas values of LVSP, dp/dt_{max}, and dp/dt_{min} were significantly reduced in DOX-treated rats compared to control rats (Fig. 3a–d). On the other hand, levels of CK-MB and BNP 45 and values of LVEDP were significantly reduced and values of LVSP, dp/dt_{max}, and dp/dt_{min} were significantly increased in DOX + AG-treated rats compared to DOX-treated group (Fig. 3a–d).

Histology Examination

Light microscopic examination of sample heart section of AG-treated control rats showed the normal appearance of the cardiac muscles histology that is almost similar to control rats with normal branching of cardiac muscle fibers with central oval euchromatic nuclei (Fig. 4a and b). However, DOX-treated rats showed the area of disorientation of the wavy muscles fibers with loss of the normal striation, increased spaces between myofibers, fragmentation and cytoplasmic vacuolization of the muscles fibers, congestion

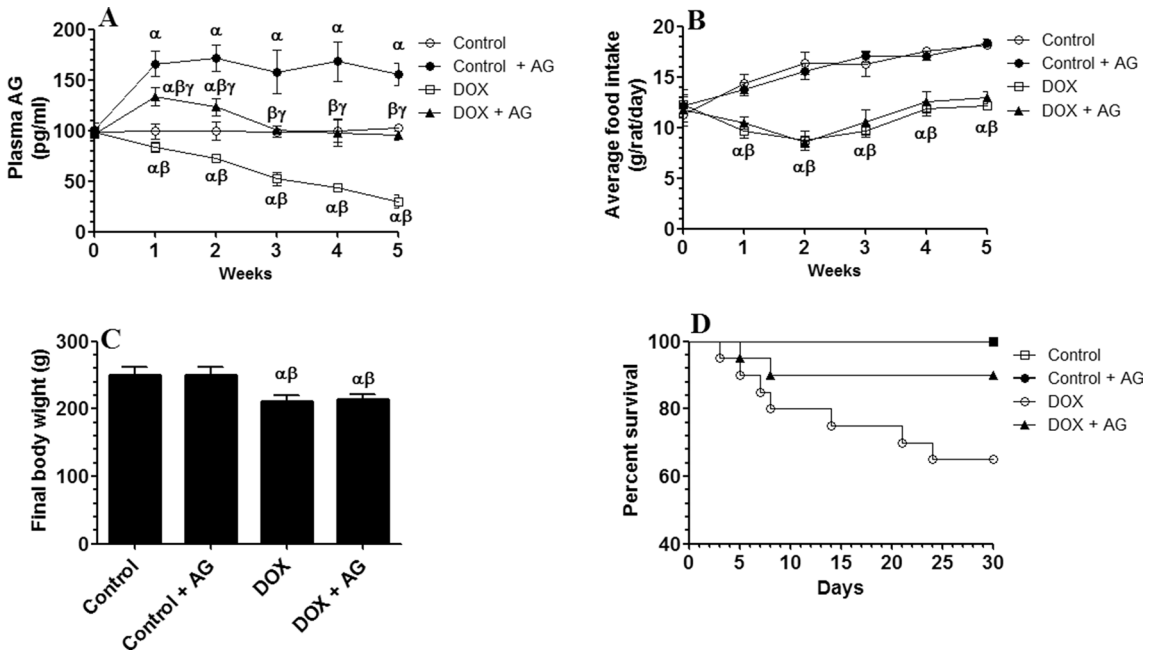

Fig. 2 Plasma levels of acylated ghrelin (**a**), average weekly food intake (**b**) and final body weights (**c**), and survival rate (**d**), of all experimental rats. Data are presented as mean ± SD of n = 12 rats/group. α: significantly different compared with the control group. β: significantly different compared with the control + AG-treated group, γ: significantly different compared with doxorubicin (DOX)-treated group

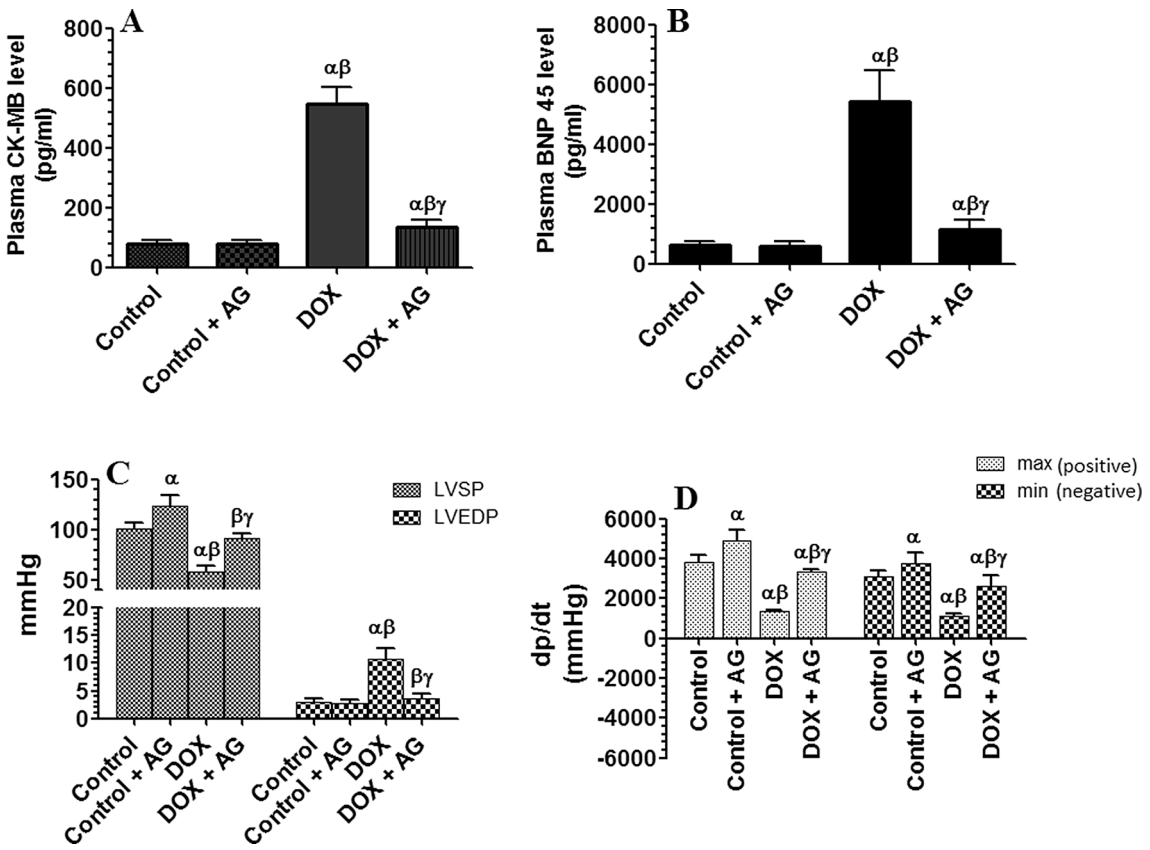

Fig. 3 Plasma levels of creatinine kinase-MB (CK-MB, **a**) and brain natriuretic peptide (BNP 54, **b**), and cardiac hemodynamic parameters (**c** and **d**) in all experimental rats. Data are presented as mean ± SD of n = 12 rats/group. α: significantly different compared with the control group. β: significantly different compared to the control + AG-treated group, γ: significantly different compared to doxorubicin (DOX)-treated group

of blood vessels, and loss of normal oval nuclei shape with most of these nuclei to undergo pyknosis and karyorrhexis (Fig. 4c). Concomitant administration of AG with DOX significantly abolished the damaging effect of DOX-on heart structure where they gain their normal striation and nuclei appearance. In these hearts, extra spaces between the muscles fibers, vacuolization, and fragmentation were barely shown (Fig. 4d). In addition, the number of pyknotic nuclei was significantly decreased.

Changes in Plasma Levels of GH and IGF-1 and Left Ventricular mRNA Levels GHRSa1, IGF-1, and SERCA2a

Plasma levels of GH and IGF-1 and cardiac mRNA levels of GHRSa1, IGF-1, and SERCA2a were significantly increased in control + AG-treated rats (Fig. 5a–d). However, plasma levels of GH and mRNA of GHSRa1 were significantly increased but plasma levels and cardiac mRNA levels of IGF-1 and SERCA2a were significantly decreased in DOX-treated rats (Fig. 5a–d). As compared to DOX-treated rats, administration of AG to DOX-treated rats resulted in the maximum increase in plasma levels of GH and significantly increased mRNA levels of SERCA2a with no alteration in mRNA levels IGF-1 and GHSR1a (Fig. 5a–d).

Changes in Left Ventricular Activity of Ca^{+2}/ Calcineurin/NFAT-4 Axis

Left ventricular (LV) protein levels of cleaved caspase-8, cleaved caspase-3 and nuclear levels of NFAT-4, as well as levels of ROS and $[Ca^{2+}]i$, and activity of calcineurin were not significant between control or control + AG (Fig. 6a–d). However, protein levels of Fas and FasL were significantly decreased and cytoplasmic protein content of NFAT-4 was significantly increased in LVs of control + AG compared to control rats (Fig. 6a). However, levels of all these measured biochemical endpoints with increased nuclear accumulation of NFAT-4 were seen in LVs of DOX-treated rats compared to control and were significantly reduced in LVs of DOX + AG-treated rats compared to DOX-treated rats (Fig. 6a–d).

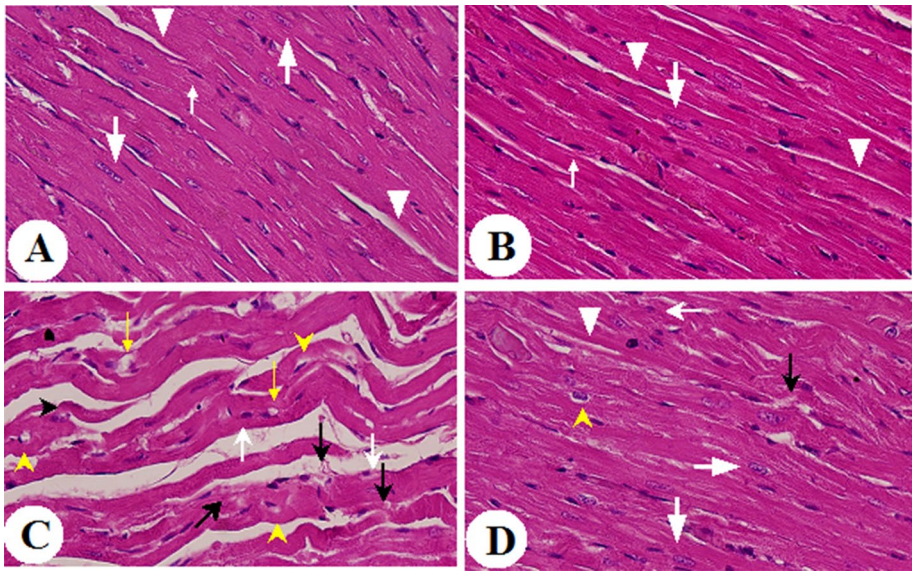

Fig. 4 Representative images of some heart samples of the hematoxylin and eosin (H&E) staining from all experimental rats. **a** and **b** were taken from control and control + acylated ghrelin (AG) treated-rats, respectively, and showing normal branching of cardiac muscle fibers (white arrowheads) with central oval euchromatic nuclei (big white arrows). The fibroblasts were seen in the endomycium, and their flat nuclei were deeply stained (small white arrows). **c** was taken from a DOX-treated rat showing disorientation of muscles fibers that appear wavy with evidence of some degeneration and fragmentation (black arrows). Multiple vacuolation was seen in the muscle fibers (yellow arrows). Multiple nuclei were pyknotic (white arrow), and some were karyorrhexis (black arrowhead). A white area surrounding the pyknotic nuclei was also seen and was abundant (yellow arrowheads). **d** was taken form DOX + AG-treated rats and showing significant improvement in muscle fibers striation which almost looks like the control (white arrowhead). Vaculation was almost not seen in muscle fibers. Most nuclei were oval in shape (big white arrows). However, very few nuclei were pyknotic (small white arrow). Also, the white areas surrounding the pyknotic nuclei were rarely seen (yellow arrowhead). Fragmentation was also seen but occasionally (black arrow)

Changes in Levels of SERCA2a and PLB and Activities of PKA and Akt

Total protein levels of PLB, Akt, and PKA were not significantly changed between all tested groups (Fig. 7a, c, d). Protein levels of SERCA2a, p-Akt (Ser^{437}) and p-PKA (Thr^{197}) were significantly increased in LVs of control + AG-treated rats but were significantly reduced in DOX-treated rats compared to control rats (Fig. 7a–d). Administration of AG to DOX-treated rats significantly increased levels of SERCA2a, p-Akt (Ser^{437}) and p-PKA (Thr^{197}) compared to control groups (Fig. 7a–d).

Cell Viability, Calcineurin Activity, and $[Ca^{2+}]i$ Levels in Cultured Adult Cardiomyocytes

Cell viability of cultured cardiomyocytes and their calcineurin activity and $[Ca^{2+}]i$ were not affected in AG-treated cells compared to control cells treated with diluted DMSO (0.1%) (Fig. 8a–c). On the other hand, calcineurin activity and $[Ca^{2+}]i$ levels were significantly decreased and cell viability was significantly decreased in DOX-treated cells compared to control cells and were reversed when DOX-treated cells were coincubated with AG (Fig. 8a–c). Interestingly, cell viability, calcineurin activity and $[Ca^{2+}]i$ levels were not significantly different between DOX-treated cells and DOX + AG pre-incubated with AG receptor antagonist (D-Lys3-GHRP-6), Akt inhibitor (VIII), or PKA inhibitor (KT-5720) (Fig. 8a–c).

Protein Levels of SERCA2a, FasL, p-PBL (Ser16 and Thr17), and Cleaved Caspase-8 in Cultured Adult Cardiomyocytes

Protein levels of FasL and cleaved caspase-8 were significantly increased and protein levels of SERCA2a and p-PBL (Ser^{16} and Thr^{17}) were significantly decreased in DOX-treated cells (Fig. 9a–d). On the other hand, protein levels of FasL and cleaved caspase-8 were significantly decreased whereas protein levels of SERCA2a and p-PBL (Ser^{16} and Thr^{17}) were significantly increased in cultured cardiomyocytes incubated with diluted DMSO and AG (Control + AG) or DOX + AG treated cells (Fig. 9a–d). Pre-incubating the DOX + AG with AG receptor antagonist (D-Lys3-GHRP-6), Akt inhibitor (VIII), or PKA inhibitor (KT-5720) completely abolished the effect of AG and the levels of these parameters were similar to those seen in DOX-treated cells (Fig. 9a–d).

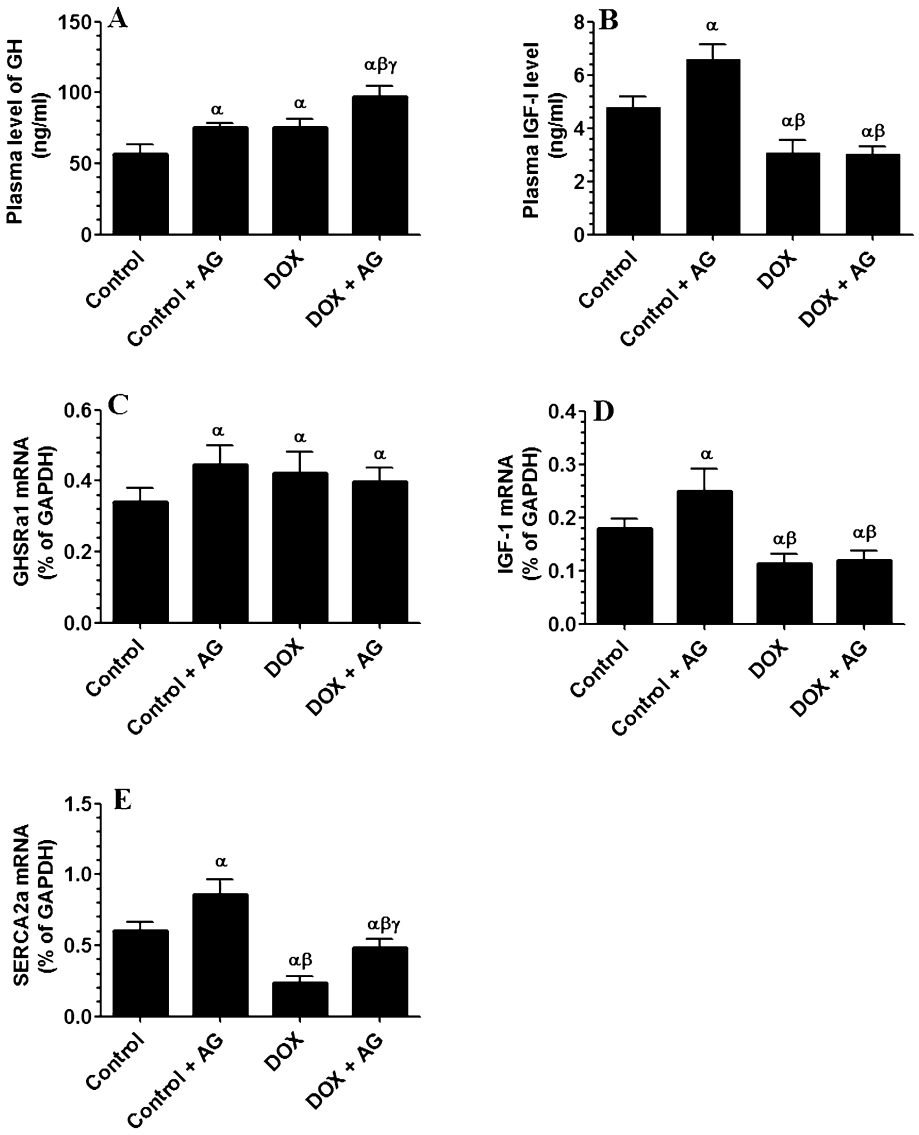

Fig. 5 Plasma levels of growth hormones (GH, **a**) and insulin-like growth factor-1 (IGF-1, **b**) and mRNA levels of GHSRa1 (**c**), IGF-1 (**d**), SERCA2a (**e**) in all experimental rats. Data are presented as mean ± SD of n = 6 rats/group. α: significantly different compared with the control group. β: significantly different compared to the control + AG-treated group, γ: significantly different compared to doxorubicin (DOX)-treated group

Changes in Ultrastructure Changes

Compared to control rats, administration of AG to control rats did not cause any alteration in the ultrastructure of the LVs cells and similar picture to that of control rats was seen (Fig. 10a and b). However, DOX-therapy resulted in severe damage of the LVs including degenerated cytoplasm, damaged myofibrils fragmentation of Z and H muscle bands and damaged mitochondria. In addition, it resulted in it in small pyknotic nuclei with the fragmentation of chromatin masses in their nuclear envelopes (Fig. 10c). On the other hand, administration of AG to DOX-treated rats significantly improved LVs cells ultrastructure, restored muscle fibers mass, cells striation and improved mitochondria structure (Fig. 10d).

Discussion

This in vivo study is the first in the literature that showed that DOX is associated with reduced SERCA2a levels and activity, as well as, lower phosphorylation of PLB at Ser^{16} and Thr^{17}. In addition, it is uniquely showed that AG could prevent DOX-induced Fas/FasL apoptosis by restoring Ca^{2+} homeostasis and inhibits NFAT-4 nuclear accumulation by reversing the above-mentioned mechanisms through activation of PKA and Akt.

It has been demonstrated that DOX therapy is associated with multi-organ toxicity including bone marrow depression and cardiac, pulmonary, hepatic, renal, and testicular toxicity [41–43]. In this, regards, it was shown that short-term DOX administration in rodents (up to 10 days) is associated

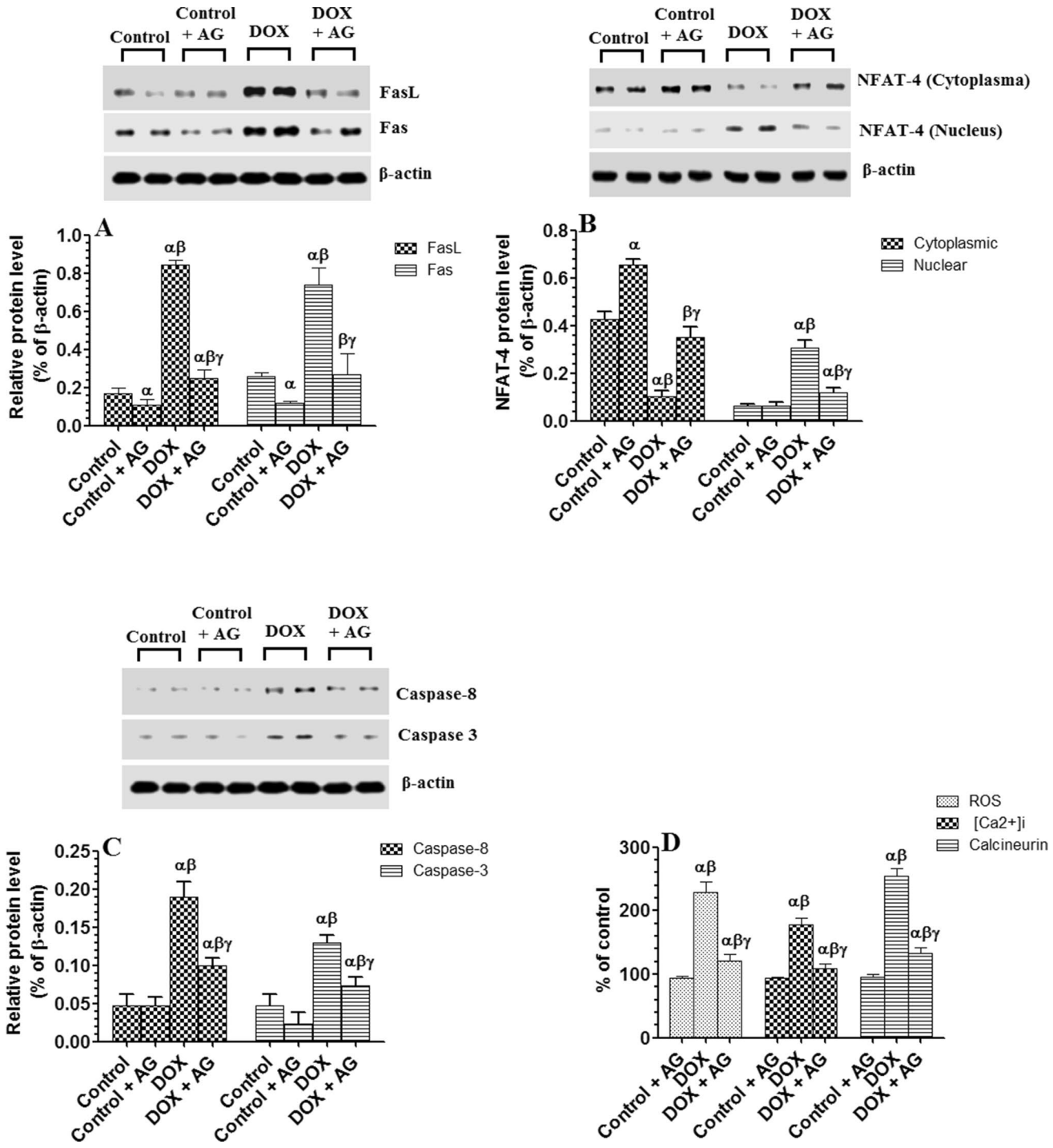

Fig. 6 Protein levels Fas and Fas ligand (FasL) (**a**), cleaved caspase-8 and 3 (**c**), levels of reactive oxygen species (ROS, **d**) and intracellular calcium [Ca^{2+}]i (**d**), and activity of calcineurin (**d**) in the total left ventricular (LV) homogenates, as well as, LV cytoplasmic and nuclear levels of NFAT-4 (**b**) in all experimental rats. Data are presented as mean ± SD of n = 6 rats/group. α: significantly different compared with the control group. β: significantly different compared to the control + AG-treated group, γ: significantly different compared to doxorubicin (DOX)-treated group

with renal and hepatic toxicity, whereas cardiac toxicity and congestive HF can develop at least 3 weeks post the last dose of DOX and is associated with depressed cardiac function, ascites, hepatomegaly, congested liver, and increased mortality (30%) [31, 44]. Similar to these findings, DOX-treated rats of this study had a mortality rate of 35% and

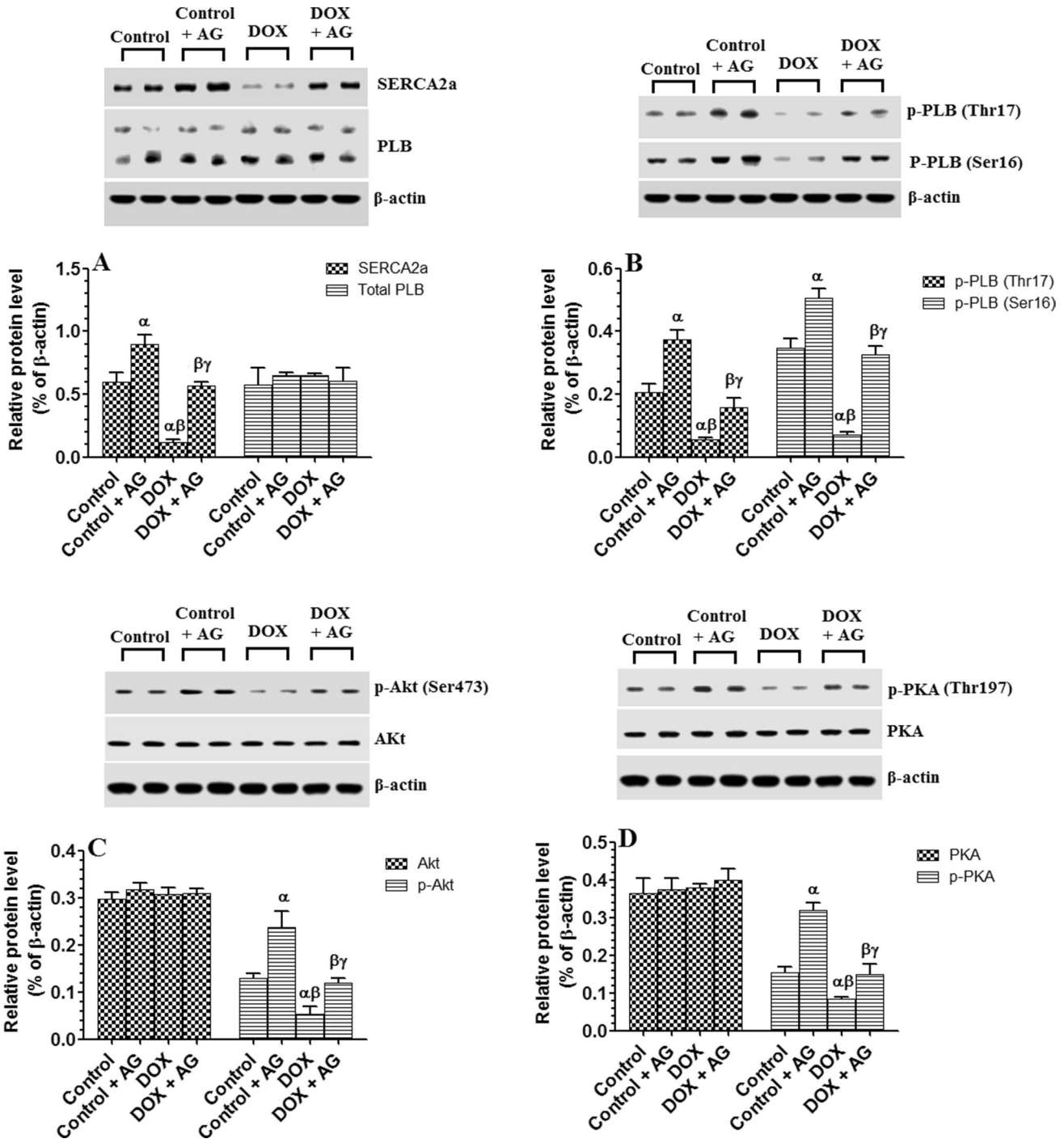

Fig. 7 Protein levels SERCA2a (**a**), total phospholamban (PLB) (**a**), phosph-phospholamban (p-PLB Ser[16] and Thr[17] (**b**) total levels of Akt and phospho-Akt (Ser[473]) (**c**) and total PKA and phospho PKA (Thr[197]) (**d**) in left ventricles (LVs) of all experimental rats. Data are presented as mean ± SD of n = 6 rats/group. α: significantly different compared with the control group. β: significantly different compared to the control + AG-treated group, γ: significantly different compared to doxorubicin (DOX)-treated group

demonstrated several signs of cardiac toxicity 3 weeks post the last dose of DOX including depressed systolic function, increased LVEDP, vacuolation of the myocytes, myofibrillar loos, mitochondria damage, the higher circulatory levels of CK-MB and Troponin T, ascites, and hepatomegaly. All these alterations have been previously described in failing hearts of both human and animals after DOX therapy and were attributed to increased generation of ROS, impaired $[Ca^{+2}]i$ overload, and active apoptosis [31, 44–49]. In addition, we have also observed a significant reduction in rat's

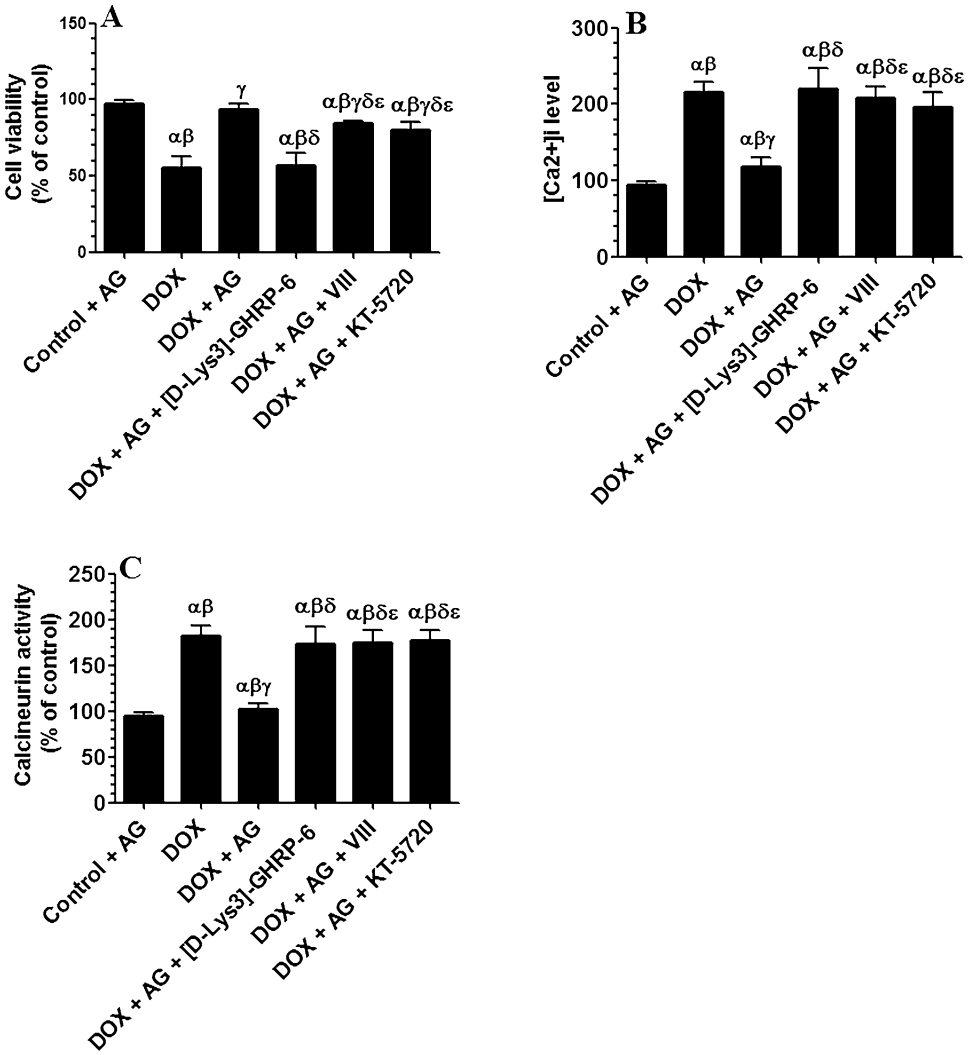

Fig. 8 Cell viability (**a**), levels of intracellular calcium [Ca^{2+}]i (**b**) and activity of calcineurin (**c**) in cultured adult cardiomyocytes under various treatments. Cells were incubated in the culture media with DOX (1 μM) in the absence or presence of AG (1 μM) for 20 h. Control cells were incubated with diluted DMSO (0.1%). Ghrelin receptor antagonist ([D-Lys3]-GHRP-6; 10 μM), Akt inhibitor (VIII; 20 μM), or PKA inhibitor (KT-5720; 5 μ) were added for 2 h before changing the media with a new one containing DOX and AG. Data are presented as mean ± SD of n = 6 rats/group. α: significantly different compared with the control group. β: significantly different compared to the control + AG-treated group, γ: significantly different compared to doxorubicin (DOX)-treated group

final body weights after DOX therapy which could be attributed to the DOX-induced reduction in food intake and appetite as demonstrated previously in this animal model [50].

On the other hand, patients or animal's models of HF usually have lower plasma levels of AG compared to control and the severity of HF correlates with the decrease in circulatory AG [51–53]. Hence, we hypothesized that restoring normal levels of AG could prevent DOX-induced cardiotoxicity. In the same line, the circulatory levels of AG were dropped significantly starting from week 1 post DOX therapy and reach the peak at the end of week 5. However, the selected dose of AG in this study significantly increased AG in control and DOX-rats by 60–70% and prevented the decrease in AG in DOX-treated rats during all weeks of this study. In fact, the levels of AG in DOX-treated rats were completely normalized by such AG regimen. Similar to these findings, AG at this dose was shown to cause physiological increase in the circulatory levels of AG in rats without any influence on food intake [33, 34]. This could explain why control + AG or DOX + AG-treated rats had normal food intake and weight gain and could suggest that all these cardiac benefits (as discussed below) afforded by AG are independent on food intake or modulating body weight.

However, the cardioprotective effect of AG was demonstrated in the hearts of both control and DOX-treated rats. Opposite to DOX-treated rats, coadministration of AG along with DOX for 35 days significantly increased rat's survival rate, reduced the observed gross abnormalities (ascites and hepatomegaly) and improved hemodynamic functions of DOX-treated rats. It also increased systolic function of the hearts of control rats. In addition, based on our observations, the DOX + AG was healthier and more energetics during all weeks of the study. Similar to these findings, the stimulatory effect of AG on heart contractility of healthy men has been also shown previously [23]. Further support for the protective effect of AG against DOX-induced cardiotoxicity was evident by the lower circulatory levels of cardiac markers, morphology and structure and lower levels of cleaved caspase-3, as a marker of apoptosis, in the LVs of DOX + AG-treated rats, effects that were independent of food intake.

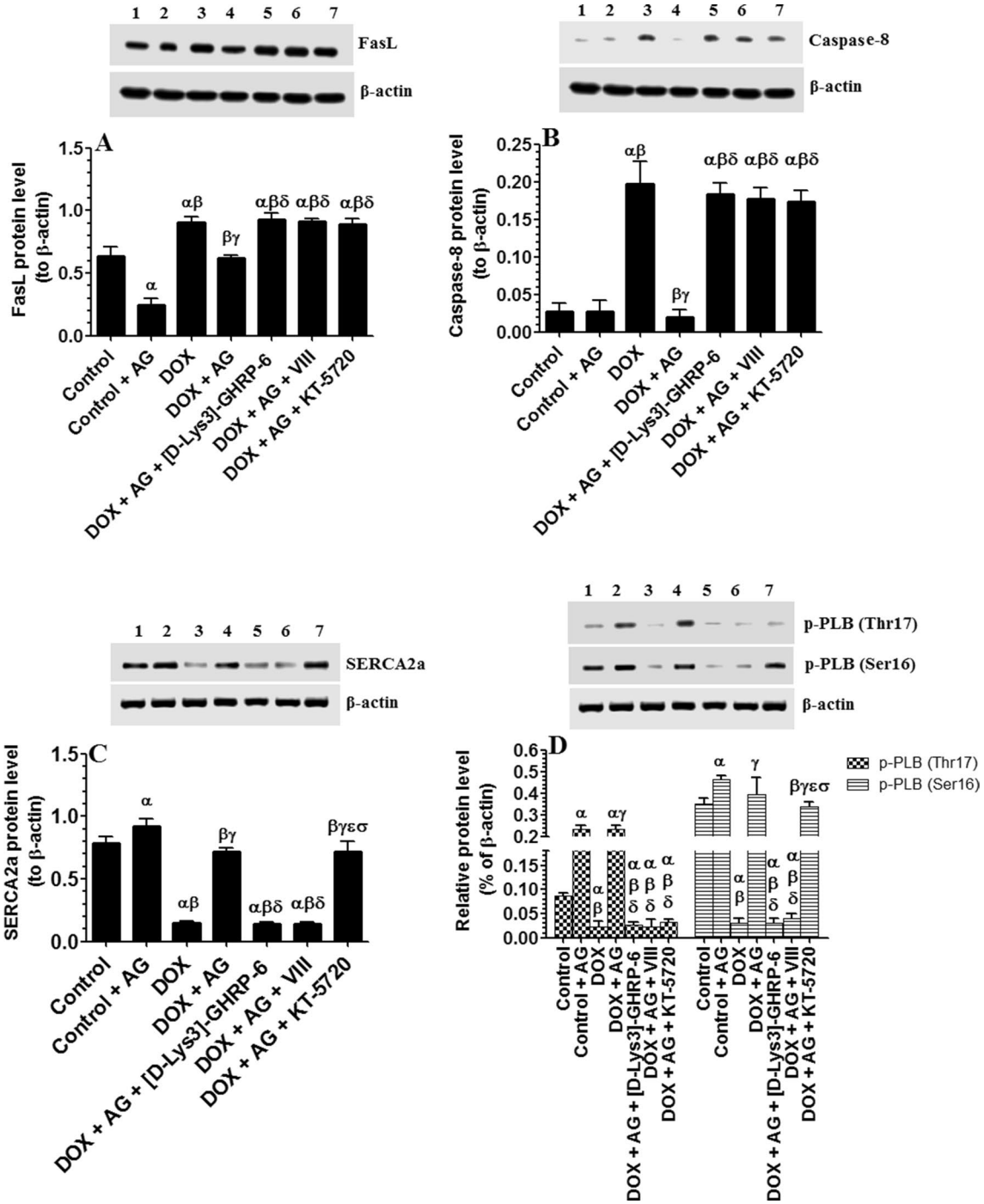

Fig. 9 Protein levels of fas ligand (FasL, **a**), cleaved caspase-8 (**b**), SERCA2a (**c**), and phospho-phospholamban (p-PLB Ser^{16} and Thr^{17}) (**d**) in cultured adult cardiomyocytes under various treatments. Cells were incubated in the culture media with DOX (1 μM) in the absence or presence of AG (1 μM) for 20 h. Control cells were incubated with diluted DMSO (0.1%). Ghrelin receptor antagonist ([D-Lys3]-GHRP-6; 10 μM), Akt inhibitor (VIII; 20 μM), or PKA inhibitor (KT-5720; 5 μ) were added for 2 h before changing the media with a new one containing DOX and AG. Data are presented as mean ± SD of n = 6 rats/group. α: significantly different compared with the control group. β: significantly different compared to control + AG-treated group, γ: significantly different compared to doxorubicin (DOX)-treated group

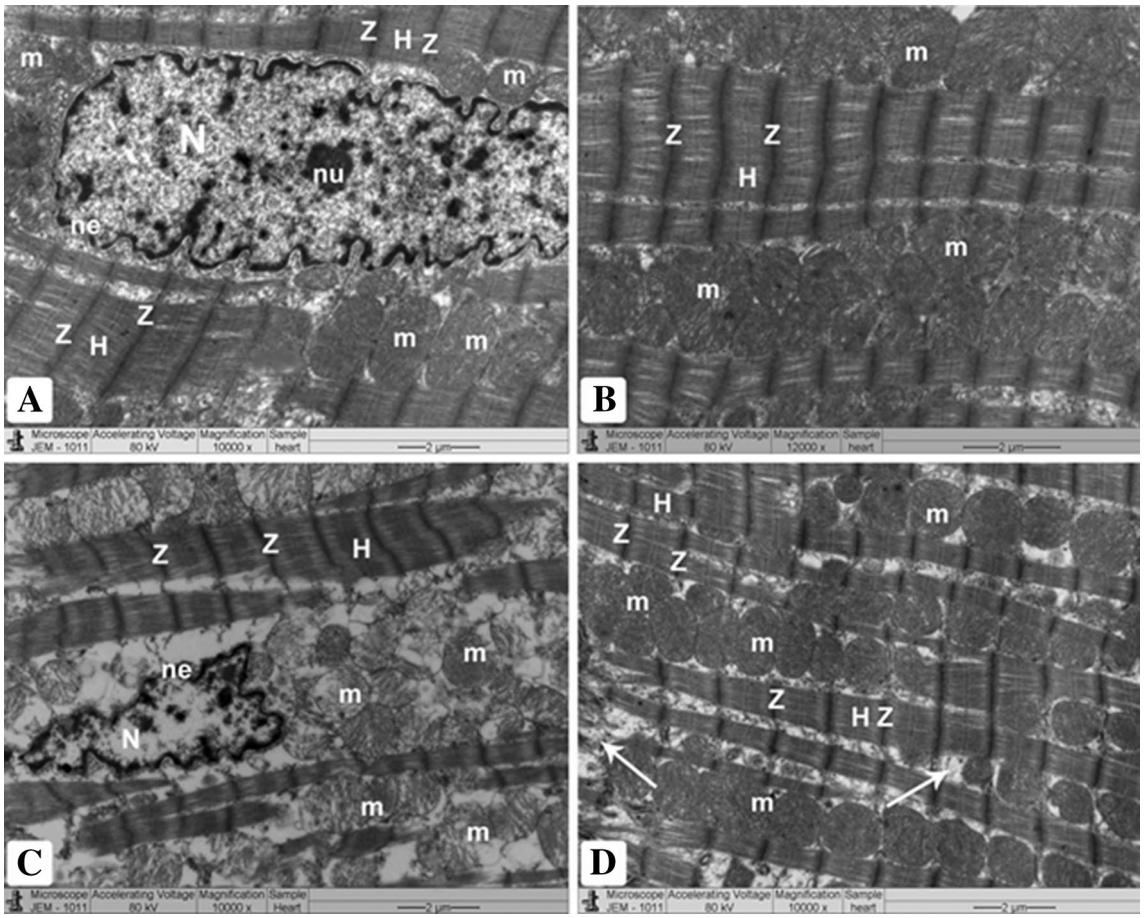

Fig. 10 Transmission electron (TEM) micrographs of myocardial tissues of all experimental groups. **a** and **b** taken from the control and control + AG-treated groups, respectively. They are showing normal myocardial tissue with normal striated heart muscle fibers, mitochondria (m) and a clear nuclear (N) and muscle bands (Z and H bands). Each nucleus (N) surrounded by the nuclear envelope (ne) and contained nucleolus (nu) and chromatin masses. **c** taken from the DOX-treated rats and showing apoptotic myocardial cells. Degenerated cytoplasm with damaged myofibrils was also seen. Fragmentation of muscle bands (Z and H bands) and mitochondria (m) were also observed. Small pyknotic nuclei (N) with the fragmentation of chromatin masses on their nuclear envelopes (ne) were seen in these apoptotic cells. **d** taken from the DOX + AG-treated rats and showing improvement of myocardial tissue with normal striated heart muscle fibers, mitochondria (m) and muscle bands (Z and H bands). Focal damage between myocardial fibers (arrows) was also seen

However, the mechanisms by which DOX and AG induce cardiac damage and protection, respectively, remain largely unknown, and need further investigation. Activation of calcineurin/NFAT4 is common in the cardiomyocytes chronically treated DOX and is associated with upregulation of FasL and activation of Fas/FasL-mediated apoptosis and is induced by intracellular levels of ROS and Ca^{2+} [5]. Generally, NFAT is a group of cytoplasmic proteins that usually sequestered in the cytoplasm as they are phosphorylated [5]. However, their nuclear translocation and the transcriptional activity are enhanced by calcineurin. All NFAT members (NFAT1-4) have been previously described in the hearts of rats [54]. On the other hand, current evidence is showing that AG is able to inhibit Fas agonist-induced extrinsic cell death [27, 28]. Interestingly, the protective effect of AG on cardiac function, cardiac enzymes, mortality rate, histopathological and ultrastructural abnormalities was associated with a reduction in the intracellular levels of ROS and Ca^2, which could be related to inhibition of NFAT4/FasL pathway.

Indeed, DOX-treated hearts of the current study showed a significant increase in the activity of calcineurin, nuclear accumulation of NFAT, and increased levels of FasL, all of which were completely reversed by co-administration of AG. Similar inhibitory effects of AG on calcineurin activity and FasL levels were also reported in the DOX-treated adult cultured cardiomyocytes of the in vitro part of this study. Remarkably, this effect was completely abolished in DOX + AG-treated cells pre-incubated with ghrelin receptor antagonist ([D-Lys3]-GHRP-6), Akt inhibitor (VIII), or PKA inhibitor (KT-5720). All these findings prompted us to conclude that the mechanism of protection of AG against

DOX-induced cardiac apoptosis and improvement in cardiac function involve inhibition of $[Ca^{+2}]i$ activation of PKA and Akt and mediated through GHSRa1.

An interesting observation is the ability of AG to inhibit Fas and FasL expressions in the LVs of control of healthy rats. This was associated with a significant reduction in basal levels of ROS and an increase in the the accumulation of NFAT-4 in the cytoplasmic fraction. Hence, it may be an important question of how does AG result in all these changes without affecting $[Ca^{+2}]i$ level or calcineurin activity? In this regard, it is important to mention that NFAT activity is not only regulated by calcineurin but also by other kinases which can phosphorylate NFAT in the cytoplasm or in the nucleus, thus inhibiting their nuclear translocation or increase their nuclear export and so increasing their cytoplasmic levels. Among these are GS3K, members of MAPK (P38, JNK, and ERK1/2) and mOTR. Hence, it could be possible that AG increased the cytoplasmic levels of NFAT-4 and hence decreased FasL levels by modulating the activity of any of these kinases. In addition, it was previously shown that the transcription and expression of Fas in DOX-treated cardiomyocytes is related to the redox state and is largely induced by ROS [7]. Similar findings were also reported in hypoxic hearts [55]. Ghrelin was shown to improve the antioxidant defense system in the heart of animals [23], which explains the decrease in ROS observed in the heart of control + AG-treated rats. Such a decrease in ROS may explain the reduction in Fas receptor expression in the LV of these rats.

For this reason, we targeted the effect of DOX and AG on the activity of SERCA2a pump given its functional role in Ca^{+2} mobilizations during the contraction and relaxation of the mammalian heart. In this regards, it is important to mention that the activity of SERCA2a is normally induced by increasing the level of their expression and phosphorylation by PLB [15]. PBL activity itself is activated by direct phosphorylation through PKA, CAMKII, and Akt [18, 21]. Similar to other authors [14, 15], we found a significant decrease in mRNA and protein levels of SERCA2a in DOX-treated LVs as well as in DOX-treated cultured adult cardiomyocytes. What is considered unique and novel in this study is that we are the first to show that DOX induces inhibition of PLB activity by decrease phosphorylation rate of PLB at Ser^{16} and Thr^{17} without altering PBL total levels. This has prompted us to go further and investigate the effect of DOX on activities of PKA and Akt which can phosphorylate PBL at Ser^{17} as well as at Ser^{16} and Thr^{17}, respectively. As expected, DOX significantly lowered the activity of both enzymes as shown by the decreased p-PKA (Thr^{197}) and p-Akt (Ser^{473}). This could be an additive to the existing mechanisms by which DOX disturbs cardiac Ca^{2+} homeostasis. Supporting to our findings, DOX-induced cardiac toxicity was associated with inhibition of PI3K/Akt signaling pathway and restoration of this signal rescued the hearts of animals from DOX-induced cardiac damage and HF [56–59]. Moreover, PKA-dependent regulatory proteins are significantly reduced in the failing hearts of animals [60, 61].

On the contrary, AG significantly increased mRNA and protein levels of SERCA2a in the LVs, as well as in cultured cardiomyocytes of both control and DOX-treated, suggesting a regulatory role of AG on SERCA2a synthesis. This effect was completely abolished by pre-incubating the cells with the AG receptor antagonist ([D-Lys3]-GHRP-6) or with the Akt inhibitor (VIII) but not with PKA inhibitor (KT-5720). Based on these findings and the lower activity of Akt and levels of SERCA2a in the LVs of DOX-treated rats, these finding may suggest a crucial role of Akt in the regulation of SERCA2a levels. However, this needs further investigation. In addition, if the effect of AG on SERCA2a is also mediated by inhibition of ERK1/2-Erg1 was not studied here and needs further research.

In addition, chronic administration of AG to healthy or DOX-treated rats as well as to control or DOX-treated cultured cardiomyocytes significantly increased activity of PKA and Akt and increased PBL activity by increasing its phosphorylation at Ser^{16} and Thr^{17}, an effect that was abolished with all inhibitors used. To the best of our knowledge, this is the first study to show this effect in the heart of animals which may explain the previously reported increase in heart contractility in healthy males and in patients with HF [23]. Indeed, the anti-apoptotic and cardioprotective effect of AG was shown to involve activation of PI3K/Akt signaling pathway, thus confirming the importance of this pathway in AG cardioprotection [27].

On the other hand, AG is known to mediate its cardioprotection by increasing levels of GH and subsequent release of IGF-1 from periphery and synthesis in the heart [24]. Receptors of both and IGF-1, as well as mRNA of IGF, have been detected in mammalian's cardiomyocytes [24]. Both GH and IGF-1 exert numerous cardioprotective functions in the heart including increase contractility and inhibition of apoptosis [24]. Hence, it was of our interest to investigate if the cardioprotective effect of AG, observed in this study, is dependent or independent of modulating growth hormone (GH)/IGF axis.

Even this could be possible in the hearts of healthy rats as evident by the significant increase in circulatory levels of GH and IGF-1 and higher mRNA of cardiac IGF-1, data of this study confirmed that the above mentioned cardioprotective effects of AG against DOX-induced cardiac damage and HF are completely independent of GH/IGF-1 axis. Growth hormone levels were significantly increased in the plasma of the DOX-treated rats and increased further after concomitant administration of AG. Such increase in Plasma levels of GH has been also shown in animal's models of HF or in patients

who died from HF and was attributed as a compensatory mechanism to maintain heart function and structure [24, 62, 63]. However, circulatory levels and cardiac mRNA levels of IGF-1 were significantly reduced in DOX or DOX + AG-treated rats with no significant variation between the two. These findings have been also reported in previous studies in rodents or patients with HF and have been explained by the existence of GH resistance [24, 62, 63].

Overall, the findings of this study suggest that AG could be a novel therapeutic agent against DOX-induced cardiotoxicity. However, Further studies are needed to confirm this effect in clinical trials. This is urgently needed to replace the available dioxopiperazine compounds which are currently used to mitigate DOX-induced cardiotoxicity and were shown to have numerous adverse effects [64]. Indeed, Dexrazoxane is one of the most common dioxopiperazine compounds that is currently used to prevent anthracycline-based chemotherapy due to its rapid passage into the cells, forming an EDTA-like form, ADR-925, which is a potent iron chelator, and being a strong catalytic inhibitor of DNA topoisomerase II [64, 65]. In spite of its cardiac protection, phase 1 and II cardioprotection studies have shown that Dexrazoxane is associated with myelotoxicity (neutropenia and thrombocytopenia), the reversible elevation of hepatic transaminases, increased urinary excretion of iron and zinc, mucositis nausea, vomiting, and alopecia. In addition, Dexrazoxane increased in the incidence of second primary malignancies by three fold in pediatric patients [66–71].

On the other hand, at all tested doses published in most clinical studies, AG was shown with an excellent safety report with very few side effects [72]. However, the major side effects reported with higher dose of AG (10.0 µg/kg) and included transient flushing in the majority of the participant (10%), gastric rumbles (2.3%), and neurocognitive effects including somnolence, fatigue, change in mood, and vertigo (2.8%) [72–75]. In addition, AG is associated with increasing lipogenesis and hyperglycemia in patients [72, 76]. In addition, it can decrease gastric pH and circulatory levels of sex hormones including FSH and LH [72, 77, 78]. Also, AG inhibited sympathetic nervous system and affected the sleep pattern [72, 79, 80]. Hence, further clinical studies should be conducted to test the safety of AG in DOX cancer patients.

In conclusion, the findings of this study clearly show that chronic administration of AG at a supra-physiological dose is able to restore normal levels of AG in DOX-treated rats. Such an effect is cardioprotective that is able to prevent alterations Ca^{2+} hemostasis by increasing levels and activity of SERCA2a directly or through phosphorylation inhibition of PLB. Together, these ultimately lead to increase cardiac contractility and inhibits NFAT4 nuclear accumulation and upregulation of FasL and thus Fas/FasL-mediated cell death. Based on these observations, our recommendation is to keep eyes on circulatory levels of AG in cancer patients during DOX therapy and to translate the findings of this study into clinical practice.

Acknowledgments The authors would like to thank the Animal facility staff at the King Khalid University (KKU), Abha, KSA for their help in taking care of animals, providing treatment, and arranging blood tissue collection. They would like also to thank the Physiology and Biochemistry technical staff at the College of Medicine at KKU for their contribution in the recording of the cardiovascular function of the experimental groups and helping in determination of some biochemical parameters. Furthermore, the authors would like to thank Dr. Reffat Eid, the Head of the Electron Microscope unit at the College of Medicine in the KKU for his significant contribution in the histology and electron microscopy studies. The authors extend their appreciation to the Deanship of Scientific Research at King Khalid University for funding this work through the research group program under Grant Number (R.G.P.1/40/39).

Funding This study was funded by the Deanship of Scientific Research at King Khalid University, Abha, Saudi Arabia (Grant Number R.G.P.1/40/39).

Compliance with Ethical Standards

Conflict of interest The authors declare no conflict of interest.

References

1. Shi, J., Abdelwahid, E., & Wei, L. (2011). Apoptosis in anthracycline cardiomyopathy. *Current Pediatric Reviews, 7,* 329–336.
2. Thorn, C. F., Oshiro, C., Marsh, S., Hernandez-Boussard, T., McLeod, H., Klein, T. E., et al. (2011). Doxorubicin pathways: Pharmacodynamics and adverse effects. *Pharmacogenetics and Genomics, 21,* 440–446.
3. Wallace, K. B. (2007). Adriamycin-induced interference with cardiac mitochondrial calcium homeostasis. *Cardiovascular Toxicology, 7,* 101–107.
4. Niu, J., Azfer, A., Wang, K., Wang, X., & Kolattukudy, P. E. (2009). Cardiac-targeted expression of soluble Fas attenuates doxorubicin-induced cardiotoxicity in mice. *Journal of Pharmacology and Experimental Therapeutics, 328,* 740–748.
5. Kalivendi, S. V., Konorev, E. A., Cunningham, S., Vanamala, S. K., Kaji, E. H., Joseph, J., et al. (2005). Doxorubicin activates nuclear factor of activated T-lymphocytes and Fas ligand transcription: Role of mitochondrial reactive oxygen species and calcium. *Biochemical Journal, 389,* 527–539.
6. Tsutamoto, T., Wada, A., Maeda, K., Mabuchi, N., Hayashi, M., Tsutsui, T., et al. (2001). Relationship between plasma levels of cardiac natriuretic peptides and soluble Fas: Plasma soluble Fas as a prognostic predictor in patients with congestive heart failure. *J Card Fail., 7,* 322–328.
7. Yamaguchi, S., Suzuki, T., Okuyama, M., Nitobe, J., Nakamura, N., Mitsui, Y., et al. (2000). Apoptosis in rat cardiac myocytes induced by Fas ligand: Priming for Fas-mediated apoptosis with doxorubicin. *Journal of Molecular and Cellular Cardiology, 32,* 881–889.
8. Wehrens, X. H., & Marks, A. R. (2004). Novel therapeutic approaches for heart failure by normalizing calcium cycling'. *Nature Reviews Drug Discovery, 3,* 565–573.
9. Schmidt, U., Hajjar, R. J., Helm, P. A., Kim, C. S., Doye, A. A., & Gwathmey, J. K. (1998). Contribution of abnormal sarcoplasmic

reticulum ATPase activity to systolic and diastolic dysfunction in human heart failure. *Journal of Molecular and Cellular Cardiology., 30,* 1929–1937.
10. Schmidt, U., Hajjar, R. J., Kim, C. S., Lebeche, D., Doye, A. A., & Gwathmey, J. K. (1999). Human heart failure: cAMP stimulation of SR Ca(2+)-ATPase activity and phosphorylation level of phospholamban. *American Journal of Physiology, 277,* H474–H480.
11. Marks, A. R. (2013). Calcium cycling proteins and heart failure: Mechanisms and therapeutics. *The Journal of Clinical Investigation, 123,* 46–52.
12. Seth, M., Sumbilla, C., Mullen, S. P., Lewis, D., Klein, M. G., Hussain, A., et al. (2004). Sarco(endo)plasmic reticulum Ca^{2+}ATPase (SERCA) gene silencing and remodeling of the Ca^{2+} signaling mechanism in cardiac myocytes. *Proceedings of the National academy of Sciences of the United States of America, 101,* 16683–16688.
13. Dodd, D. A., Atkinson, J. B., Olson, R. D., Buck, S., Cusack, B. J., Fleischer, S., et al. (1993). Doxorubicin cardiomyopathy is associated with a decrease in calcium release channel of the sarcoplasmic reticulum in a chronic rabbit model. *J Clin Invest., 91,* 1697–1705.
14. Arai, M., Tomaru, K., Takizawa, T., Sekiguchi, K., Yokoyama, T., Suzuki, T., et al. (1998). Sarcoplasmic reticulum genes are selectively down-regulated in cardiomyopathy produced by doxorubicin in rabbits. *Journal of Molecular and Cellular Cardiology, 30,* 243–254.
15. Arai, M., Yoguchi, A., Takizawa, T., Yokoyama, T., Kanda, T., Kurabayashi, M., et al. (2000). Mechanism of doxorubicin-induced inhibition of sarcoplasmic reticulum Ca21-ATPase Gene transcription. *Circulation Research, 86,* 8–14.
16. Tada, M. (2003). Calcium cycling proteins of the cardiac sarcoplasmic reticulum. *Circulation Journal, 67,* 729–737.
17. Vangheluwe, P., Sipido, K. R., Raeymaekers, L., & Wuytack, F. (2006). New perspectives on the role of SERCA2′s Ca^{2+} affinity in cardiac function. *Biochimica et Biophysica Acta, 1763,* 1216–1228.
18. Fearnley, C. J., Roderick, H. L., & Bootman, M. D. (2011). Calcium signaling in cardiac myocytes. *Cold Spring Harbor Perspectives in Biology, 3,* a004242.
19. Jo, S. H., Leblais, V., Wang, P. H., Crow, M. T., & Xiao, R. P. (2002). Phosphatidylinositol 3-kinase functionally compartmentalizes the concurrent G(s) signaling during beta2-adrenergic stimulation. *Circulation Research, 91,* 46–53.
20. Gao, M. H., Tang, T., Guo, T., Miyanohara, A., Yajima, T., Pestonjamasp, K., et al. (2008). Adenylyl cyclase type VI increases Akt activity and phospholamban phosphorylation in cardiac myocytes. *The Journal of Biological Chemistry., 283,* 33527–33535.
21. Catalucci, D., Latronico, M. V., Ceci, M., Rusconi, F., Young, H. S., Gallo, P., et al. (2009). Akt increases sarcoplasmic reticulum Ca^{2+} cycling by direct phosphorylation of phospholamban at Thr17. *The Journal of Biological Chemistry, 284,* 28180–28187.
22. Zhang, Y., Chen, Y., Zhang, M., Tang, Y., Xie, Y., Huang, X., et al. (2014). Doxorubicin induces sarcoplasmic reticulum calcium regulation dysfunction via the decrease of SERCA2 and phospholamban expressions in rats. *Cell Biochemistry and Biophysics, 70,* 1791–1798.
23. Zhang, G., Yin, X., Qi, Y., Pendyala, L., Chen, J., Hou, D., et al. (2010). Ghrelin and cardiovascular diseases. *Current Cardiology Reviews, 6,* 62–70.
24. Eid, R. A., Alkhateeb, M. A., Eleawa, S., Al-Hashem, F. H., Al-Shraim, M., El-Kott, A. F., et al. (2018). Cardioprotective effect of ghrelin against myocardial infarction-induced left ventricular injury via inhibition of SOCS3 and activation of JAK2/STAT3 signaling. *Basic Research in Cardiology, 113,* 13.
25. Gnanapavan, S., Kola, B., Bustin, S. A., Morris, D. G., McGee, P., Fairclough, P., et al. (2002). The tissue distribution of the mRNA of ghrelin and subtypes of its receptor, GHS-R, in humans. *Journal of Clinical Endocrinology and Metabolism, 87,* 2988.
26. Iglesias, M. J., Piñeiro, R., Blanco, M., Gallego, R., Diéguez, C., Gualillo, O., et al. (2004). Lago F growth hormone releasing peptide (ghrelin) is synthesized and secreted by cardiomyocytes. *Cardiovascular Research, 62,* 481–488.
27. Baldanzi, G., Filigheddu, N., Cutrupi, S., Catapano, F., Bonissoni, S., Fubini, A., et al. (2002). Ghrelin and des-acyl ghrelin inhibit cell death in cardiomyocytes and endothelial cells through ERK1/2 and PI 3-kinase/AKT. *Journal of Cell Biology, 159,* 1029–1037.
28. Xu, Z., Lin, S., Wu, W., Tan, H., Wang, Z., Cheng, C., et al. (2008). Ghrelin prevents doxorubicin-induced cardiotoxicity through TNF-alpha/NF-kappaB pathways and mitochondrial protective mechanisms. *Toxicology, 247,* 133–138.
29. Fang, H., Hong, Z., Zhang, J., Shen, D. F., Gao, F. F., Sugiyama, K., et al. (2012). Effects of ghrelin on the intracellular calcium concentration in rat aorta vascular smooth muscle cells. *Cellular Physiology and Biochemistry., 30,* 1299–1309.
30. Han, D., Huang, W., Ma, S., Chen, J., Gao, L., Liu, T., et al. (2015). Ghrelin improves functional survival of engrafted adipose-derived mesenchymal stem cells in ischemic heart through PI3K/Akt signaling pathway. *BioMed Research International*. https://doi.org/10.1155/2015/858349.
31. Lou, H., Danelisen, I., & Singal, P. K. (2005). Involvement of mitogen-activated protein kinases in adriamycininduced cardiomyopathy. *The American Journal of Physiology-Heart and Circulatory Physiology, 288,* 1925–1930.
32. Dallak, M. (2018). Acylated ghrelin induces but deacylated ghrelin prevents hepatic steatosis and insulin resistance in lean rats: Effects on DAG/PKC/JNK pathway. *Biomedicine & Pharmacotherapy, 105,* 299–311.
33. Li, Y., Hai, J., Li, L., Chen, X., Peng, H., Cao, M., et al. (2013). Administration of ghrelin improves inflammation, oxidative stress, and apoptosis during and after non-alcoholic fatty liver disease development. *Endocrin., 43,* 376–386.
34. Işeri, S. O., Sener, G., Saglam, B., Ercan, F., Gedik, N., & Yeğen, B. C. (2008). Ghrelin alleviates biliary obstruction-induced chronic hepatic injury in rats. *Regulatory Peptides, 146,* 73–79.
35. Donthi, R. V., Huisamen, B., & Lochner, A. (2000). Effect of vanadate and insulin on glucose transport in isolated adult rat cardiomyocytes. *Cardiovascular Drugs and Therapy, 14,* 463–470.
36. Pentassuglia, L., Heim, P., Lebboukh, S., Morandi, C., Xu, L., & Brink, M. (2016). Neuregulin-1β promotes glucose uptake via PI3K/Akt in neonatal rat cardiomyocytes. *American Journal of Physiology Endocrinology and Metabolism, 310,* E782–E794.
37. Dong, J., Gao, C., Liu, J., Cao, Y., & Tian, L. (2016). TSH inhibits SERCA2a and the PKA/PLN pathway in rat cardiomyocytes. *Oncotarget, 7,* 39207–39215.
38. Xu, J., Han, Q., Shi, H., Liu, W., Chu, T., & Li, H. (2017). Role of PKA in the process of neonatal cardiomyocyte hypertrophy induced by urotensin II. *International Journal of Molecular Medicine, 40,* 499–504.
39. Frutos, M. G., Cacicedo, L., Méndez, C. F., Vicent, D., González, M., & Sánchez-Franco, F. (2007). Pituitary alterations involved in the decline of growth hormone gene expression in the pituitary of aging rats. *Journals of Gerontology Series A Biological Sciences and Medical Sciences, 62,* 585–597.
40. Buehlmeyer, K., Doering, F., Daniel, H., Petridou, A., Mougios, V., Schulz, T., et al. (2007). IGF-1 gene expression in rat colonic mucosa after different exercise volumes. *Journal of Sports Science and Medicine, 6,* 434–440.
41. Zhao, X., Zhang, J., Tong, N., Chen, Y., & Luo, Y. (2012). Protective effects of berberine on doxorubicin-induced hepatotoxicity in mice. *Biological &/and Pharmaceutical Bulletin, 35*(5), 796–800.

42. Mohan, M., Kamble, S., Gadhi, P., & Kasture, S. (2010). Protective effect of *Solanum torvum* on doxorubicin-induced nephrotoxicity in rats. *Food and Chemical Toxicology, 4,* 436–440.
43. Jensen, R. A., Acton, E. M., & Peters, H. (1984). Doxorubicin cardiotoxicity in the rat: Comparison of electrocardiogram, transmembrane potential, and structural effect. *Journal of Cardiovascular Pharmacology, 6,* 186–200.
44. Siveski-Iliskovic, N., Kaul, N., & Singal, P. K. (1994). Probucol promotes endogenous antioxidants and provides protection against adriamycin-induced cardiomyopathy in rats. *Circulation, 89,* 2829–2835.
45. Childs, A. C., Phaneuf, S. L., Dirks, A. J., Phillips, T., & Leeuwenburgh, C. (2002). Doxorubicin treatment in vivo causes cytochrome C release and cardiomyocyte apoptosis, as well as increased mitochondrial efficiency, superoxide dismutase activity, and Bcl-2: Bax ratio. *Cancer Research, 62,* 4592–4598.
46. Miyata, S., Takemura, G., Kosai, K., Takahashi, T., Esaki, M., Li, L., et al. (2010). Anti-Fas gene therapy prevents doxorubicin-induced acute cardiotoxicity through mechanisms independent of apoptosis. *American Journal of Pathology, 176,* 687–698.
47. Tian, S., Hirshfield, K. M., Jabbour, S., Toppmeyer, D., Haffty, B. G., Khan, A. J., et al. (2014). Serum biomarkers for the detection of cardiac toxicity after chemotherapy and radiation therapy in breast cancer patients. *Frontiers in Oncology, 4,* 277.
48. Chatterjee, K., Zhang, J., Honbo, N., & Karlinerb, J. S. (2010). Doxorubicin cardiomyopathy. *Cardiology, 115,* 155–162.
49. Mitry, M. A., & Edwards, J. G. (2016). Doxorubicin induced heart failure: Phenotype and molecular mechanisms. *International Journal of Cardiology Heart & Vasculature., 10,* 17–24.
50. Warpe, V. S., Mali, V. R., Arulmozhi, S., Bodhankar, S. L., & Mahadik, K. R. (2015). Cardioprotective effect of ellagic acid on doxorubicin induced cardiotoxicity in wistar rats. *Journal of Acute Medicine, 5,* 1–8.
51. Nagaya, N., Uematsu, M., Kojima, M., Ikeda, Y., Yoshihara, F., Shimizu, W., et al. (2001). Chronic administration of ghrelin improves left ventricular dysfunction and attenuates development of cardiac cachexia in rats with heart failure. *Circulation, 104,* 1430–1435.
52. Chen, Y., Ji, X. W., Zhang, A. Y., Lv, J. C., Zhang, J. G., & Zhao, C. H. (2014). Prognostic value of plasma ghrelin in predicting the outcome of patients with chronic heart failure. *Archives of Medical Research, 45,* 263–269.
53. Khatib, M. N., Shankar, A., Kirubakaran, R., Agho, K., Simkhada, P., Gaidhane, S., et al. (2015). Effect of ghrelin on mortality and cardiovascular outcomes in experimental rat and mice models of heart failure: A systematic review and meta-analysis. *PLoS ONE, 10,* e0126697.
54. Pu, W. T., Ma, Q., & Izumo, S. (2003). NFAT transcription factors are critical survival factors that inhibit cardiomyocyte apoptosis during phenylephrine stimulation in vitro. *Circulation Research, 92,* 725–731.
55. Tanaka, M., Ito, H., Adachi, S., Akimoto, H., Nishikawa, T., Kasajima, T., et al. (1994). Hypoxia induced apoptosis with enhanced expression of Fas antigen messenger RNA in cultured neonatal rat cardiomyocytes. *Circulation Research, 75,* 426–433.
56. Venkatesan, B., Prabhu, S. D., Venkatachalam, K., Mummidi, S., Valente, A. J., Clark, R. A., et al. (2010). WNT1-inducible signaling pathway protein-1 activates diverse cell survival pathways and blocks doxorubicin-induced cardiomyocyte death. *Cellular Signalling, 22,* 809–820.
57. Das, J., Ghosh, J., Manna, P., & Sil, P. C. (2011). Taurine suppresses doxorubicin-triggered oxidative stress and cardiac apoptosis in rat via up-regulation of PI3-K/Akt and inhibition of p53, p38-JNK. *Biochemical Pharmacology, 81,* 891–899.
58. Lee, B. S., Oh, J., Kang, S. K., Park, S., Lee, S. H., Choi, D., et al. (2015). Insulin protects cardiac myocytes from doxorubicin toxicity by Sp1-mediated transactivation of surviving. *PLoS ONE*. https://doi.org/10.1371/journal.pone.0135438.
59. Yu, W., Sun, H., Zha, W., Cui, W., Xu, L., Min, Q., et al. (2017). Apigenin attenuates adriamycin-induced cardiomyocyte. Apoptosis via the PI3K/AKT/mTOR pathway. *Evidence-Based Complementary and Alternative Medicine, 25,* 90676. https://doi.org/10.1155/2017/2590676.
60. Piddo, A. M., Sánchez, M. I., Sapag-Hagar, M., Corbalán, R., Foncea, R., Ebensperger, R., et al. (1996). Cyclic AMP-dependent protein kinase and mechanical heart function in ventricular hypertrophy induced by pressure overload or secondary to myocardial infarction. *Journal of Molecular and Cellular Cardiology, 28,* 1073–1083.
61. Zakhary, D. R., Moravec, C. S., Stewart, R. W., & Bond, M. (1999). Protein kinase A (PKA)-dependent troponin-I phosphorylation and PKA regulatory subunits are decreased in human dilated cardiomyopathy. *Circulation, 99,* 505–510.
62. Anand, I., Ferrari, R., Kalra, G., Wahi, P., Poole-Wilson, P., & Harris, P. (1989). Edema of cardiac origin: Studies of body water and sodium, renal function, hemodynamic indexes and plasma hormones in untreated congestive cardiac failure. *Circulation, 80,* 299–305.
63. Friberg, L., Werner, S., Eggertsen, G., & Ahnve, S. (2000). Growth hormone and insulin-like growth factor-1 in acute myocardial infarction. *European Heart Journal, 21,* 1547–1554.
64. Langer, S. W. (2014). Dexrazoxane for the treatment of chemotherapy-related side effects. *Cancer Manag Res., 6,* 357–363.
65. Hasinoff, B. B., Kuschak, T. I., Yalowich, J. C., & Creighton, A. M. (1995). A QSAR study comparing the cytotoxicity and DNA topoisomerase II inhibitory effects of bisdioxopiperazine analogs of ICRF-187 (dexrazoxane). *Biochemical Pharmacology, 50*(7), 953–958.
66. Holcenberg, J. S., Tutsch, K. D., Earhart, R. H., et al. (1986). Phase I study of ICRF-187 in pediatric cancer patients and comparison of its pharmacokinetics in children and adults. *Cancer Treatment Reports, 70*(6), 703–709.
67. Liesmann, J., Belt, R., Haas, C., & Hoogstraten, B. (1981). Phase I evaluation of ICRF-187 (NSC-169780) in patients with advanced malignancy. *Cancer, 47*(8), 1959–1962.
68. Vogel, C. L., Gorowski, E., Davila, E., et al. (1987). Phase I clinical trial and pharmacokinetics of weekly ICRF-187 (NSC 169780) infusion in patients with solid tumors. *Investigational New Drugs, 5*(2), 187–198.
69. Marty, M., Espié, M., Llombart, A., Monnier, A., Rapoport, B. L., & Stahalova, V. (2006). Dexrazoxane Study Group multicenter randomized phase III study of the cardioprotective effect of dexrazoxane (Cardioxane) in advanced/metastatic breast cancer patients treated with anthracycline-based chemotherapy. *Annals of Oncology, 17*(4), 614–622.
70. Mouridsen, H. T., Langer, S. W., Buter, J., et al. (2007). Treatment of anthracycline extravasation with Savene (dexrazoxane): Results from two prospective clinical multicentre studies. *Annals of Oncology, 18*(3), 546–550.
71. Tebbi, C. K., London, W. B., Friedman, D., et al. (2007). Dexrazoxane-associated risk for acute myeloid leukemia/myelodysplastic syndrome and other secondary malignancies in pediatric Hodgkin's disease. *Journal of Clinical Oncology, 25,* 493–500.
72. Garin, M. C., Burns, C. M., Kaul, S., & Cappola, A. R. (2013). The human experience with ghrelin administration. *Journal of Clinical Endocrinology and Metabolism, 98*(5), 1826–1837.
73. Adachi, S., Takiguchi, S., Okada, K., et al. (2010). Effects of ghrelin administration after total gastrectomy: A prospective, randomized, placebo-controlled phase II study. *Gastroenterology, 138,* 1312–1320.

74. Hiura, Y., Takiguchi, S., Yamamoto, K., et al. (2012). Fall in plasma ghrelin concentrations after cisplatin-based chemotherapy in esophageal cancer patients. *Int J Clin Oncol., 17,* 316–323.
75. Lambert, E., Lambert, G., Ika-Sari, C., et al. (2011). Ghrelin modulates sympathetic nervous system activity and stress response in lean and overweight men. *Hypertension, 58,* 43–50.
76. Vestergaard, E. T., Hansen, T. K., Gormsen, L. C., et al. (2007). Constant intravenous ghrelin infusion in healthy young men: Clinical pharmacokinetics and metabolic effects. *American Journal of Physiology Endocrinology and metabolism, 292,* E1829–E1836.
77. Kluge, M., Schussler, P., Uhr, M., Yassouridis, A., & Steiger, A. (2007). Ghrelin suppresses secretion of luteinizing hormone in humans. *The Journal of Clinical Endocrinology & Metabolism, 92,* 3202–3205.
78. Kluge, M., Uhr, M., Bleninger, P., Yassouridis, A., & Steiger, A. (2009). Ghrelin suppresses secretion of FSH in males. *Clinical Endocrinology (Oxford), 70,* 920–923.
79. Huda, M. S., Mani, H., Dovey, T., et al. (2010). Ghrelin inhibits autonomic function in healthy controls, but has no effect on obese and vagotomized subjects. *Clinical Endocrinology—Oxford, 73,* 678–685.
80. Kluge, M., Schussler, P., Bleninger, P., et al. (2008). Ghrelin alone or co-administered with GHRH or CRH increases non-REM sleep and decreases REM sleep in young males. *Psychoneuroendocrinology, 33,* 497–506.